Eur. Phys. J. B **3**, 447–454 (1998)

THE EUROPEAN PHYSICAL JOURNAL B

Anharmonic dynamical behaviour in bcc zirconium

O. Dubos[1,a], W. Petry[1], J. Neuhaus[1], and B. Hennion[2]

[1] Physik Department E 13, Technische Universität München, Garching, Germany
[2] Laboratoire Léon Brillouin, CEN Saclay, France

Received: 24 December 1997 / Received in final form: 9 March 1998 / Accepted: 19 March 1998

Abstract. We present inelastic neutron scattering measurements of the low energy and strongly damped phonons in the high temperature bcc phase of zirconium. These phonons were investigated at different scattering vectors **Q** but equivalent phonon wave vectors **q** in different Brillouin zones or along different but equivalent paths in the same Brillouin zone. Neither the observed differences in intensity nor in line shapes can be explained by the coherent one-phonon scattering law $S_1(\mathbf{Q},\omega)$. This leads to an apparent violation of the fundamental symmetry of lattice dynamics. Taking into account the strong anharmonicity of these phonons, interferences between one- and multi-phonon scattering are held responsible for these effects. Measurements in different scattering planes reveal that due to the symmetry of the bcc lattice, these effects can only be observed in certain directions.

PACS. 63.20.Ry Anharmonic lattice modes – 63.20.Dj Phonon states and bands, normal modes, and phonon dispersion

1 Introduction

Most metallic elements of the periodic table crystallize in an open body centered cubic (bcc) structure and transform upon lowering the temperature or increasing pressure to close packed structures like hexagonal (hcp) or face centered cubic (fcc). These phase transformations are of first order, reconstructive in the sense that the crystal adopts a new structure, which does not belong to the same symmetry group of the parent phase, and are often called martensitic transitions. Most interesting are the transition metals of group 3 (Sc,Y,La) and 4 (Ti, Zr, Hf). Elements of both groups undergo at least one martensitic transition from their high temperature bcc or β-phase towards a low temperature hcp or α-phase. In addition to the temperature induced transition, elements of group 4 undergo at high pressure another martensitic transformation to a simple hexagonal structure (hex) called ω-phase [1]. Furthermore, they show very fast self-diffusion compared to other bcc metals or metals with hcp or fcc structures [2]. Both aspects, the tendency to undergo phase transformations and fast self-diffusion, can be related to their unusual vibrational behavior, *i.e.* low energy and temperature dependent phonons [3–5]. These phonons are also characterized by unusual strong damping. This sign of anharmonicity is to our knowledge the most important found up to now in elements of simple mono-atomic structure [6]. Therefore, these metals may serve as a model case to study experimentally and theoretically the effects of anharmonicity. In this article, we mainly concern with the experimental aspect of the study. The large coherent scattering length of zirconium, its low incoherent and absorption cross sections, favor this element for an experimental study by means of inelastic neutron scattering.

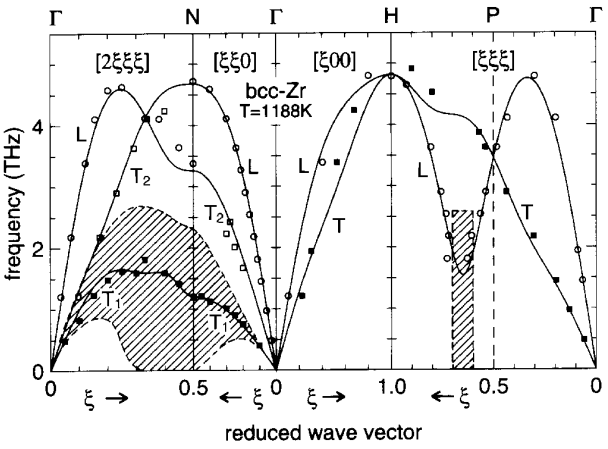

Fig. 1. Phonon dispersion of β-Zr as measured by [7]. Shaded areas represent regions of intense inelastic scattering intensity.

The phonon dispersion of β-Zr [7,8] (Fig. 1) is dominated by very unusual characteristics compared to other bcc metals like those of group 5 (V, Nb, Ta) and 6 (Cr, Mo, W). The high symmetry longitudinal phonon branch $L[\xi\,\xi\,\xi]$ shows a pronounced dip of very low

[a] e-mail: dolivier@physik.tu-muenchen.de

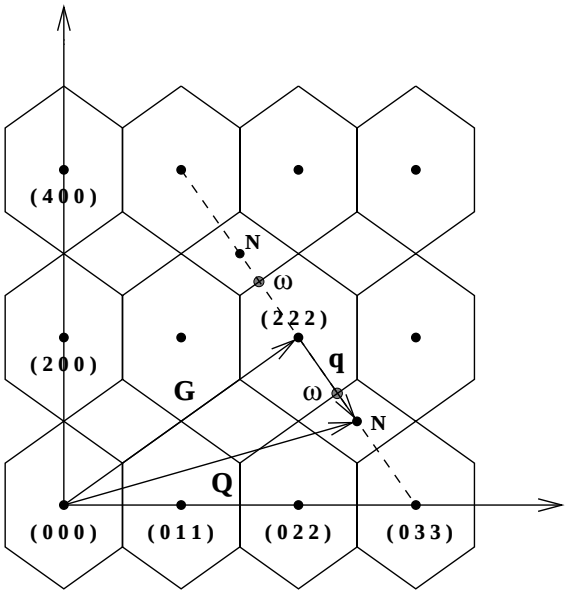

Fig. 2. Scattering geometry for measurements of the $T_1[2\xi\,\xi\,\xi]$ transverse phonon branch in the $(0\,1\,\overline{1})$ scattering plane.

energy at ξ=2/3. The displacement pattern generated by this phonon transforms the high temperature β-phase into the ω-phase. Compared to other transverse branches, the high symmetry $T_1[\xi\,\xi\,0]$ and the off symmetry $T_1[2\xi\,\xi\,\xi]$ branches are of very low energies. The zone boundary phonon $T_1\,\frac{1}{2}[1\,1\,0]$ (N-point) shuffles the stacking sequence of the $\{1\,1\,0\}_\beta$ planes into a sequence of $\{0\,0\,1\}_\alpha$ planes. However, this phonon alone is not sufficient to achieve the complete transformation. Long shear wavelength phonons are necessary to squeeze the irregular β hexagon to a regular one [9]. These long wavelength phonons can be found in the initial slope of the $T_1[2\xi\,\xi\,\xi]$ transverse branch. The symmetry of the bcc lattice implies the equivalence of the $L\,\frac{2}{3}[1\,1\,1]$ and $T_1\,\frac{1}{3}[2\,1\,1]$ phonons. Thus, the phonons necessary to undergo all phase transformations observed in Zr can be found in the off-symmetry and low energy $T_1[2\xi\,\xi\,\xi]$ transverse branch [3].

In the last two decades, there has been considerable interest in Zr or Ti alloys with elements such as V, Nb (group 5) and Cr, Mo (group 6) [10] due to the appearance of a metastable low temperature ω-phase. Extensive neutron scattering studies were performed, mostly on the ω-forming ZrNb alloys.

Diffuse scattering measurements by Moss *et al.* [11] on the diffuse ω-alloy $Zr_{0.80}Nb_{0.20}$ at room temperature ($T = 300$ K) have revealed an asymmetry in the scattering intensities in the (1 1 0) plane (Fig. 2) between the $\langle\,\overline{2}\,1\,1\,\rangle$ and $\langle\,2\,\overline{1}\,\overline{1}\,\rangle$ directions. A further asymmetry was observed in the inelastic scattering at high and room temperatures (Fig. 4 and 5 of [11]). An asymmetry in the intensities and line shapes of the $T_1[2\xi\,\xi\,\xi]$ transverse phonons measured in the same plane and along the same directions is also reported by Axe *et al.* [12] in $Zr_{0.92}Nb_{0.08}$ at $T = 965$ °C. Similar effects are observed by Noda *et al.* [13] for the $T_1[2\xi\,\xi\,\xi]$ and $T_1[\xi\,\xi\,0]$ phonons in $Zr_{0.80}Nb_{0.20}$ at room temperature in the same and other Brillouin zones of this plane. The diffuse elastic scattering intensities measured in the equivalent $(1\,\overline{1}\,0)$ plane of both $Zr_{0.985}Co_{0.015}$ and $Zr_{0.92}Nb_{0.08}$ alloys at high temperature ($T = 1273$ K) by Heiming *et al.* [14] have shown a distribution similar to the one observed by Moss *et al.* [11]. However, no asymmetry was observed for the elastic intensities in the (0 0 1) plane of both alloys. For comparison, the distribution of the elastic diffuse intensities in the $(1\,\overline{1}\,0)$ plane of pure Zr was also investigated. This distribution looks similar to those observed in both $Zr_{0.985}Co_{0.015}$ and $Zr_{0.92}Nb_{0.08}$. Provided that the coherent inelastic intensities at zero energy transfer arising from the low energy and strongly damped phonons are correctly substracted, no truly elastic intensities subsist in pure Zr. Consequently, the apparent diffuse elastic scattering intensities observed in the $(1\,\overline{1}\,0)$ plane of pure Zr which show the same asymmetry as observed in all Zr alloys are of purely inelastic origin and stem from the low energy and strongly damped phonons.

The aim of this study is to investigate in detail the low energy and strongly damped phonons with the help of inelastic neutron scattering in pure β-Zr. In particular, measurements on the $T_1[2\xi\,\xi\,\xi]$ and the $T_1[\xi\,\xi\,0]$ transverse branches and the distribution of the inelastic intensity in the $\{1\,1\,0\}$ and $\{1\,0\,0\}$ scattering planes are presented.

2 Experimental details

Rods of 10 mm diameter and 100 mm length were prepared from high-purity iodine-grade Zr bars supplied by Teledyne Wah Chang, Albany, USA. In order to access different scattering planes, several single crystals of typically 50 mm in length were grown by the zone melting technique, directly on the spectrometer. They were kept at high temperature, without intermediate cooling, by passing through a high intensity current. Crystals were grown by means of a combined measuring and crystal growth furnace [15]. The measurements were taken at the thermal three-axis spectrometer 1 T 1 at the Orphée reactor of the L.L.B in Saclay, France. All measurements were performed at constant final neutron wave vector k_f using a vertically focusing pyrolitic graphite PG (002) monochromator. For the energy analysis, we used a PG (002) or a PG (004) graphite crystal, when higher resolution was necessary, respectively. In a typical set-up, horizontal collimations of 25', 40', 40', 40' combined with a horizontally focusing analyzer and graphite filter to suppress higher order contaminations were chosen. This set-up was changed corresponding to the required scattering vectors and energy resolution. Throughout the paper, we use the convention of energy loss and gain with respect to the sample.

3 Measurements of the $T_1\,[\,2\xi\,\xi\,\xi\,]$ transverse phonon branch

Our experimental results for the $T_1\,[\,2\xi\,\xi\,\xi\,]$ branch at $T = 1333$ K are presented in Figure 3. This branch was measured in the $(0\,1\,\overline{1})$ scattering plane (Fig. 2) along the two equivalent directions $\langle\,\overline{2}\,1\,1\,\rangle$ and $\langle\,2\,\overline{1}\,\overline{1}\,\rangle$ around the (2 2 2) Brillouin zone center. For small ξ, spectra along both directions show identical intensities and line shapes. Two phonon peaks can be observed for each spectrum. At this high temperature, the difference in intensities of phonon peaks along positive and negative energy transfer can be ascribed to focusing effects and is therefore of purely instrumental nature. At large ξ, however we observed strong differences in intensities and line shapes. Strong intensities were found along the $\langle\,\overline{2}\,1\,1\,\rangle$ direction and the differences are most pronounced for $\xi = \pm 1/3$. Beyond $\xi = \pm 1/3$, when we approach the N-point ($\xi = \pm 0.5$), phonon spectra in both directions show still differences in intensity and line shape but these differences become smaller. Exactly at the N-point, line shapes in both directions are similar but intensities remain different. Similar observations are reported on the $T_1\,[\,2\xi\,\xi\,\xi\,]$ branch in the $Zr_{0.80}Nb_{0.20}$ alloy by Noda *et al.* [13] indicating the equivalence between the lattice dynamics of pure Zr and Zr alloys. It is important to note that the experimentally observed differences between the two directions can not be attributed to resolution effects. The measurements of phonon spectra at different scattering vectors imply only the rotation of the sample.

The experimental spectra can be compared with the spectra expected from the one-phonon scattering law $S_1\,(\mathbf{Q},\omega)$ for a monoatomic unit cell [16].

$$S_1\,(\mathbf{Q},\omega) = \{\,1 + n\,(\omega)\,\} \sum_{\mathbf{q}\,j} \mid F\,(\mathbf{Q},\mathbf{q}\,j)\mid^2 \times \big\{\,\delta\,(\omega - \omega_j\,(\mathbf{q})) - \delta\,(\omega + \omega_j\,(\mathbf{q}))\,\big\}, \tag{1}$$

$$\mid F\,(\mathbf{Q},\mathbf{q}\,j)\mid^2 = \frac{\hbar}{2M}\, e^{-2W_0(Q)}\, \frac{(\mathbf{Q}\cdot\mathbf{e}\,(\mathbf{q}\,j))^2}{\omega_j\,(\mathbf{q})}\,. \tag{2}$$

In the usual notation $n\,(\omega)$ represents the temperature dependent Bose occupation, $\mathbf{q}\,j$ the phonon wave vector of the j th branch ($j = 1, \cdots, 3$), $\mathbf{Q} = \mathbf{k}_i - \mathbf{k}_f$ the scattering vector. Variation with $\mathbf{Q}$ enters only in the one-phonon structure factor $F\,(\mathbf{Q},\mathbf{q}\,j)$ in terms of a Q-dependent Debye-Waller factor $e^{-2W_0(Q)}$ ($Q = \mid \mathbf{Q} \mid$) and the scalar product between $\mathbf{Q}$ and the polarization vector $\mathbf{e}\,(\mathbf{q}\,j)$. Apart from this, intensities in different Brillouin zones or by symmetry equivalent phonon wave vectors in the same Brillouin zone are identically.

The so expected variation of the scattering intensity for the $T_1\,[\,2\xi\,\xi\,\xi\,]$ phonon branch along the two equivalent directions mentioned above is depicted in Figure 4. For this calculation frequency $\omega_j\,(\mathbf{q})$ and polarization $\mathbf{e}\,(\mathbf{q}\,j)$ were obtained from the dynamical matrix, which in turn

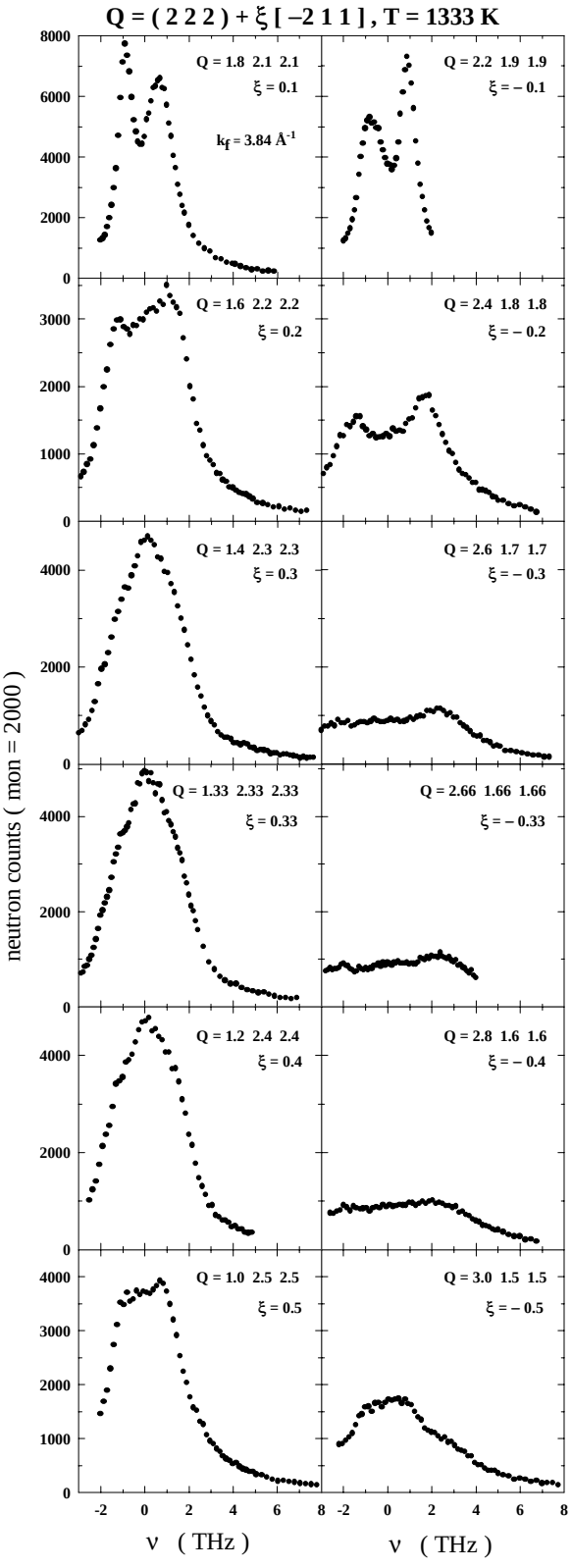

Fig. 3. Measured phonon spectra for the $T_1\,[\,2\xi\,\xi\,\xi\,]$ phonon branch. 2000 monitor counts correspond to about 40 seconds of counting time.

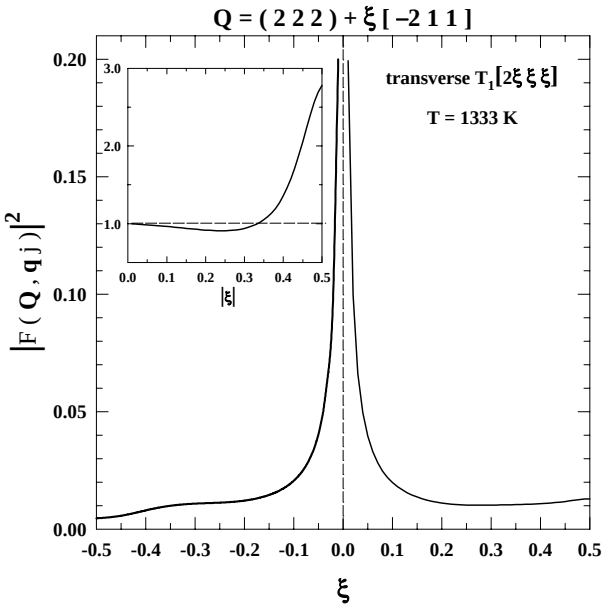

Fig. 4. Calculated variation of $\mid F(\mathbf{Q}, \mathbf{q}\,j) \mid^2$ with $\mathbf{Q}$ along the $\langle\,\overline{2}\,1\,1\,\rangle$ and $\langle\,2\,\overline{1}\,\overline{1}\,\rangle$ equivalent directions around the (2 2 2) Brillouin zone center. The inset shows the ratio of $\mid F(\mathbf{Q}, \mathbf{q}\,j) \mid^2$ between the two directions.

has been fitted to the experimental phonon frequencies in Figure 1. The insert in Figure 4 shows that for $\xi = 0$ to $\pm 1/3$ intensities are almost identically and diverge at $\xi = \pm 0.5$ by a factor 2.8. At $\xi = \pm 1/3$, both scalar products $\mathbf{Q} \cdot \mathbf{e}\,(\mathbf{q}\,j)$ and the Debye-Waller factors are identically by symmetry and therefore no intensity difference should be observed according to the one-phonon scattering law. This is in strong contradiction to our experimental findings. Particularly at $\xi = \pm 1/3$, the intensity difference between both phonons is maximized. Only for small ξ and for the high symmetry N-point ($\xi = \pm 0.5$), measured and calculated intensity roughly coincide within experimental errors.

Taking into account a finite lifetime of the phonons, the δ-functions in $S_1\,(\mathbf{Q}, \omega)$ can be replaced by a damped oscillator function [16]. In any case, the line shape of the one-phonon scattering law depends only on $\mathbf{q}\,j$ and therefore should be similar for equivalent points in reciprocal space. We conclude that the experimentally measured $\mathbf{Q}$ and ω dependences of the $T_1\,[\,2\xi\,\xi\,\xi\,]$ phonon spectra can not be explained by the one-phonon scattering law $S_1\,(\mathbf{Q}, \omega)$.

4 Measurements of the ω phonon

In the preceding measurements, the $L\,\frac{2}{3}\,[\,1\,1\,1\,]$ phonon was measured in a transverse geometry, *i.e.* we have measured the equivalent transverse phonon at $\mathbf{Q}$=(4/3 7/3 7/3) and (8/3 5/3 5/3). Now, we present measurements of this strongly damped phonon in a longitudinal geometry. For the measurements depending strongly on $\mid \mathbf{Q} \mid$, two different energy resolutions were used. High resolution

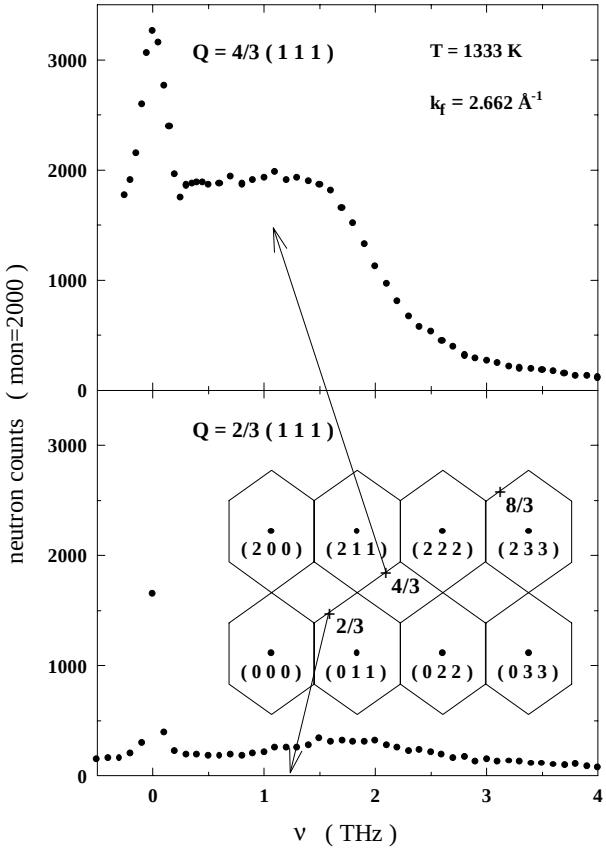

Fig. 5. Measurements of the ω-phonon at two different scattering vectors $\mathbf{Q}$=2/3(1 1 1) and 4/3(1 1 1) but equivalent phonon wave vectors $\mathbf{q}$ with $k_f = 2.662$ Å^{-1}. 2000 monitor counts correspond to about 50 seconds of counting time.

($k_f = 2.662$ Å^{-1}) was chosen to measure the $L\,\frac{2}{3}\,[\,1\,1\,1\,]$ phonon at $\mathbf{Q}$=2/3(1 1 1) and 4/3(1 1 1) (Fig. 5), whereas in order to reach $\mathbf{Q}$=8/3(1 1 1), a coarser resolution ($k_f = 4.9$ Å^{-1}) was necessary to measure the same phonon at $\mathbf{Q}$=2/3(1 1 1), 4/3(1 1 1) and 8/3(1 1 1) (Fig. 6). For both resolutions, the strongest intensities were found for the phonon spectrum measured at $\mathbf{Q}$=4/3(1 1 1). Considerable smaller intensities were found for spectra measured at $\mathbf{Q}$=2/3(1 1 1) and 8/3(1 1 1). The ratio of the different one-phonon structure factors are 1.83 between $\mathbf{Q}$=4/3(1 1 1) and 2/3(1 1 1) and 5.47 between $\mathbf{Q}$=4/3(1 1 1) and 8/3(1 1 1) respectively. It cannot explain the experimentally observed ratio of approximatively of 6 and 3 respectively. Moreover, the ratio of 3 between one-phonon structure factors at $\mathbf{Q}$=2/3(1 1 1) and 8/3(1 1 1) is in complete contradiction with the experimental observation that the stronger intensities were found at $\mathbf{Q}$=8/3(1 1 1) rather than at $\mathbf{Q}$=2/3(1 1 1). Strongly different line shapes can also be observed. The phonon spectrum at $\mathbf{Q}$=4/3(1 1 1) is very broad, considerably broader than the incoherent elastic peak which gives a measure of the energy resolution and much broader than the phonon spectrum at $\mathbf{Q}$=2/3(1 1 1). The validity of this observation at both

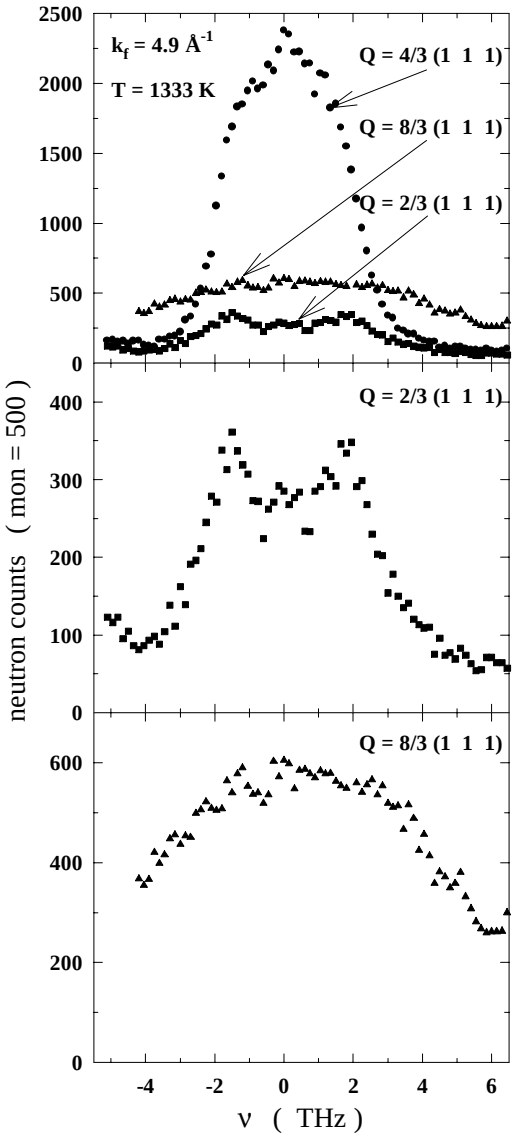

Fig. 6. Measurements of the ω-phonon at three different scattering vectors $\mathbf{Q}$=2/3(1 1 1), 4/3(1 1 1) and 8/3(1 1 1) but equivalent phonon wave vectors $\mathbf{q}$ with $k_f = 4.9$ Å^{-1}. 500 monitor counts correspond to about 160 seconds of counting time.

energy resolutions ascertains that this effect is not instrumental. At $\mathbf{Q}$=8/3(1 1 1), the intensities are smeared out, it is not possible to observe any distinct peaks.

5 Measurements of the $\mathbf{T_1\,[\,\xi\,\xi\,0\,]}$ transverse phonon branch

To investigate if similar effects can be observed for the $T_1\,[\,\xi\,\xi\,0\,]$ transverse branch, we measured this branch in the $(0\,0\,\overline{1})$ scattering plane again in different Brillouin zones and along different but equivalent directions. All scattering geometries used, (A), (B) and (C), are shown in Figure 7.

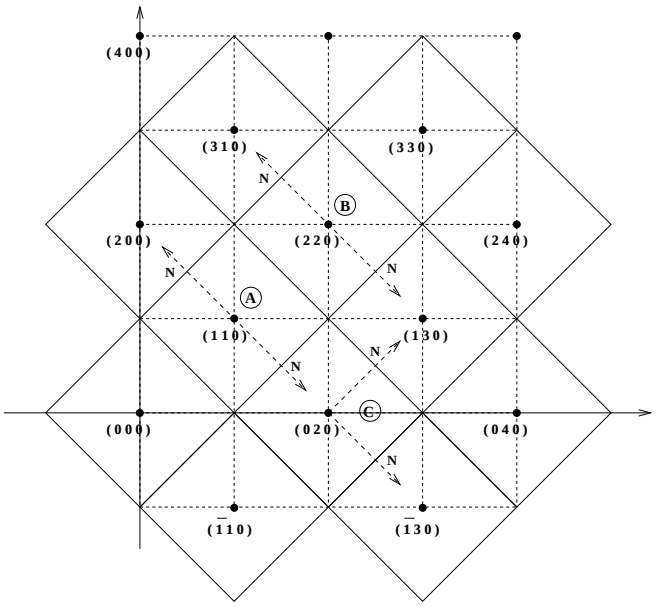

Fig. 7. The three scattering geometries used for the measurement of the $T_1\,[\,\xi\,\xi\,0\,]$ transverse phonon branch in the $(0\,0\,\overline{1})$ scattering plane.

In an examplary fashion, phonon spectra for the scattering geometry (B) are presented in Figure 8. Our results show that inside the same Brillouin zone, phonon spectra measured at different scattering vectors $\mathbf{Q}$ but equivalent phonon wave vectors $\mathbf{q}$ exhibit the same intensities and line shapes. Equivalent observations were made for geometries (A) and (C). Contrarily to the $T_1\,[\,2\xi\,\xi\,\xi\,]$ phonon branch, the $\mathbf{Q}$ and ω dependences of $T_1\,[\,\xi\,\xi\,0\,]$ phonon spectra are in complete agreement with the expected $\mathbf{Q}$ and ω dependences of the one-phonon scattering law $S_1\,(\mathbf{Q},\omega)$. Along the $[\,1\,1\,0\,]$ directions, the polarization vectors $\mathbf{e}\,(\mathbf{q}\,j)$ are given by the crystal symmetry. According to Figure 7, inside the same Brillouin zone, the scattering vectors $\mathbf{Q}$ corresponding to equivalent $\mathbf{q}$ have identical lengths. Consequently, at equivalent $\mathbf{q}$, the scalar products $\mathbf{Q}\cdot\mathbf{e}\,(\mathbf{q}\,j)$ and the Debye-Waller factors are identical and therefore the corresponding one-phonon structure factors $F\,(\mathbf{Q},\mathbf{q}\,j)$ and the one-phonon scattering law $S_1\,(\mathbf{Q},\omega)$, respectively too. Corresponding to equivalent $\mathbf{q}$, the same line shapes must be observed. More generally, the symmetry observed in the intensities and line shapes of the $T_1\,[\,\xi\,\xi\,0\,]$ phonon spectra (Fig. 8) is a direct consequence of the symmetry obeyed by the total phonon scattering law $S\,(\mathbf{Q},\omega)$, *i.e.* the point symmetry of the lattice.

6 Diffuse inelastic scattering measurements in the $(0\,1\,\overline{1})$ and $(0\,0\,\overline{1})$ planes

So far, we presented our experimental measurements of transverse $T_1\,[\,2\xi\,\xi\,\xi\,]$ phonons along two equivalent directions from one Brillouin zone center. Can we observe similar effects on this transverse phonon branch along

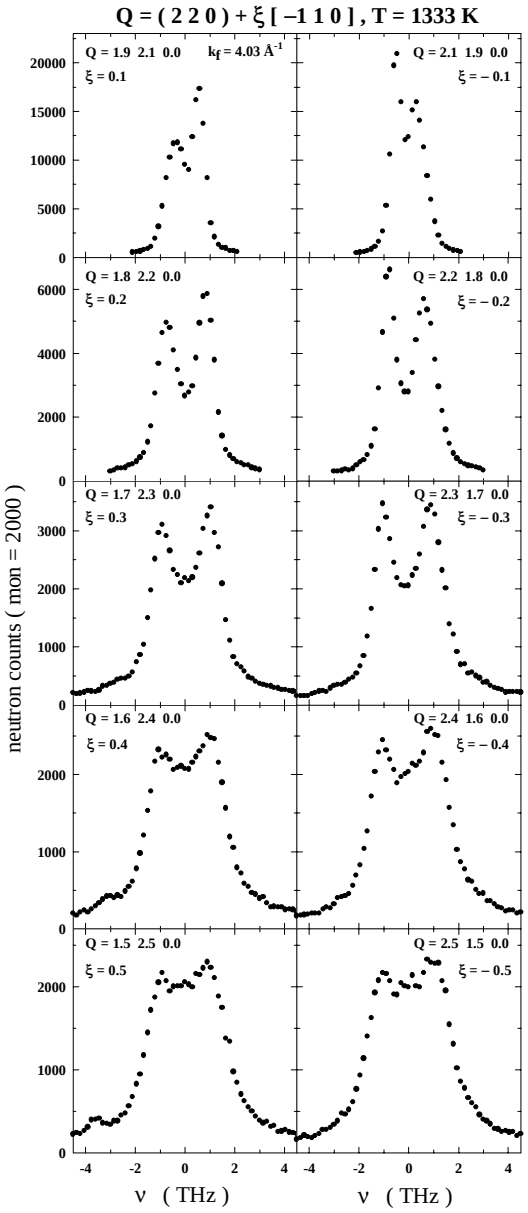

Fig. 8. Measured phonon spectra for the $T_1\,[\,\xi\,\xi\,0\,]$ phonon branch around the (2 2 0) Brillouin zone, geometry (B). 2000 monitor counts correspond to about 40 seconds of counting time.

the same directions but from different Brillouin zone centers? To obtain an overview of the dispersion surface around different Brillouin zone centers, we have measured the distribution of the inelastic scattering intensity in the $(0\,1\,\overline{1})$ plane at a frequency $\nu = 1$ THz which is presented in Figure 9. This particular energy transfer was chosen because here we expected to measure the strongest variation in phonon intensities. The distribution of inelastic scattering intensity confirms the preceding results observed on the $T_1\,[\,2\xi\,\xi\,\xi\,]$ branch measured around the (2 2 2) Brillouin zone center. Strong intensities were found along the $\langle\,\overline{2}\,1\,1\,\rangle$ direction whereas very

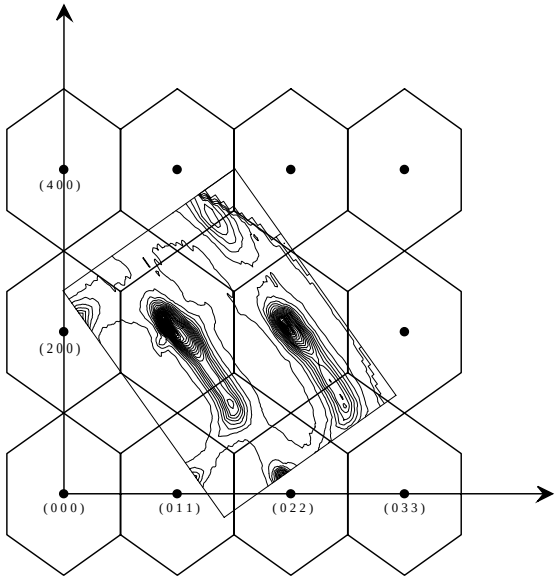

Fig. 9. Contour plot of the diffuse inelastic scattering distribution in the $(0\,1\,\overline{1})$ scattering plane at a frequency ν= 1 THz measured at $T = 1333$ K and with $k_f = 3.84$ Å^{-1}.

weak intensities were found along the opposite $\langle\,2\,\overline{1}\,\overline{1}\,\rangle$ direction. Strongest differences between the two directions were found around $\xi = \frac{1}{3}$. This point is exactly at the intersection of the two equivalent directions with the Brillouin zone boundary. These measurements reveal that the modulation in intensity is reproduced periodically in the reciprocal space. Similar distribution of inelastic scattering intensities were observed around the (2 1 1) Brillouin zone center. Summarizing, we find at each Brillouin zone always more intensity along the $\langle\,\overline{2}\,1\,1\,\rangle$ than along the $\langle\,2\,\overline{1}\,\overline{1}\,\rangle$ direction.

A similar overview of the distribution of the inelastic scattering intensity in the $(0\,0\,\overline{1})$ plane is shown in Figure 10. Here, identical intensities were found in all different but equivalent Brillouin zones and/or along all different but equivalent directions in a given Brillouin zone. Again this distribution reflects the point group property of the lattice, which determines the symmetry of the total phonon scattering law $S\,(\mathbf{Q},\omega)$. Contrarily, along the $[\,2\,1\,1\,]$ directions in the $\{\,1\,1\,0\,\}$ plane, the scattering vectors $\mathbf{Q}$ corresponding to equivalent phonon wave vectors $\mathbf{q}$ can not be related by a cubic point group symmetry operation of the lattice and are therefore not equivalent by symmetry. Consequently, phonon spectra measured at these $\mathbf{Q}$ must not have identical intensities and line shapes. Summarizing, the differences between both planes are related to their symmetry.

The diffuse inelastic intensity measured in both planes resembles very much what has been found as elastic diffuse scattering for ZrNb [11] and ZrCo [14] alloys, respectively. However, static displacement patterns in the alloys

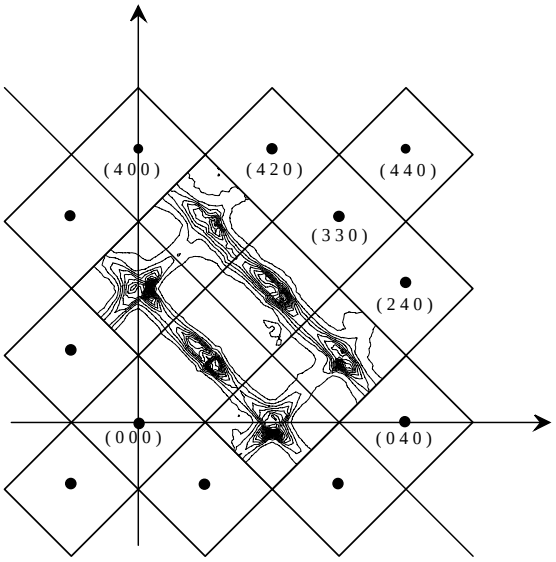

Fig. 10. Contour plot of the diffuse inelastic scattering distribution in the $(0\,0\,\overline{1})$ scattering plane at a frequency ν= 1 THz measured at $T = 1333$ K and with $k_f = 4.03$ Å^{-1}.

towards the two product phases α and ω are of purely dynamical nature in pure β-Zr.

7 Discussion

With the exception of phonon branches along high symmetry directions of the bcc structure like the $T_1\,[\,\xi\,\xi\,0\,]$ branch, our experimental results show that spectra of low energy and strongly damped phonons measured at different scattering vectors **Q** but equivalent phonon wave vectors **q** differ in intensities and line shapes. The most significant effect concerns the differences in intensities. Neither the **Q** dependence nor the ω dependence (line shape) of the one-phonon scattering law $S_1\,(\mathbf{Q},\omega)$ can explain these observations. Similar effects but much less pronounced have been observed in other bcc crystals like ^{4}He [17,18] and K [19]. Anomalies of similar importance have been reported for La [20]. Such behavior, *i.e.* low energy and strongly damped phonons as well as the asymmetry in their scattering laws, seems to be typical for systems with bcc structure and is most pronounced in the bcc phase of the group 3 and 4 transition metals.

Molecular-dynamic simulations of the coherent scattering law $S\,(\mathbf{Q},\omega)$ by Zhang *et al.* [21] in pure bcc Zr at high temperature reproduced qualitatively the anomalies observed experimentally in intensities and line shapes of the spectra at $\mathbf{Q} = 4/3(1\ 1\ 1)$ and $2/3(1\ 1\ 1)$. The asymmetry of their computed integrated scattering intensities is similar to our observation in the inelastic scattering at a frequency of 1 THz. The authors suggest that the origin of the asymmetry in the scattering lies in dynamical fluctuations between the bcc and hcp phases. Taking snapshot pictures of the atomic configuration, they identified local clusters of atoms arranged in a hcp-like configuration. The location in space and the orientation of these clusters relative to the bcc structure change with time. However, due to the dynamical nature of these fluctuations, the hcp-like arrangement of atoms is not perfect. They could reproduce the asymmetry of the scattering intensities at zero energy transfer between **Q**=(4/3 7/3 7/3) and (8/3 5/3 5/3) assuming that these intensities stem from the static scattering from clusters, in which the atoms are midway between the bcc and hcp structures. These two scattering vectors are both reciprocal lattice vectors of the hcp phase. However, this argumentation can not explain the asymmetry observed in the purely inelastic scattering around this two **Q**-vectors. Furthermore, no argument is given for the asymmetric scattering intensities at **Q**-vectors which do not correspond to hcp lattice points. We need a theory which can explain completely the asymmetry of the scattering. Strongly damped phonons are a signature of an anharmonic potential in β-Zr. Ambegaokar *et al.* [24] have shown that anharmonicity leads to interferences between one- and multi-phonon scattering. Retaining only interference between one- and two-phonon scattering and using perturbation theory in lowest order in anharmonic coefficients, Glyde [25] obtained expressions for these terms. Taking into account the two leading terms, the first one simply increases or decreases the intensities of the one-phonon scattering law $S_1\,(\mathbf{Q},\omega)$ whereas the second modifies the line shape of $S_1\,(\mathbf{Q},\omega)$. They have two interesting properties. First, they change their sign with the sign of the variable ξ. This change may explain why different intensities and line shapes of the $T_1\,[\,2\xi\,\xi\,\xi\,]$ phonon spectra are observed between the two equivalent $\langle\,\overline{2}\,1\,1\,\rangle$ and $\langle\,2\,\overline{1}\,\overline{1}\,\rangle$ directions. Second, they vanish at scattering vectors **Q** midway in between two reciprocal lattice vectors, *i.e.* at high symmetry points of the reciprocal space. Consequently, intensities and line shapes observed at the N-point ($\xi = \pm\,0.5$) are correctly explained by the one-phonon scattering law $S_1\,(\mathbf{Q},\omega)$.

We have to verify that the change of sign of both interference effects as well as their ω dependences can reproduce our experimental observations. For this purpose, numerical calculations of interference terms are necessary. Details, results as well as a comparison of these numerical calculations with our experimental data will be given in a forthcoming publication.

These experiments have been made possible by financial support of the Institut Laue-Langevin (ILL). O. D. has benefited for a thesis grant by ILL, which is gratefully acknowledged. Extensive experimental help by F. Güthoff is very much acknowledged.

References

1. J.C. Jamieson, Science **140**, 72 (1963).
2. N.L. Peterson, Comments Sol. State Phys. **8**, 53 (1978).
3. W. Petry, J. Phys. IV C2, **5** (1995).
4. W. Petry, Phase Transitions **31**, 119 (1991).
5. H.R. Schober, W. Petry, J. Trampenau, J. Phys.: Cond. Mat. **4**, 9321 (1992).
6. For an overview see Landolt-Börnstein, Volume **III**/13a, edited by K.-H. Hellwege and J.L. Olsen (Springer-Verlag Berlin, 1981).
7. A. Heiming, W. Petry, J. Trampenau, M. Alba, C. Herzig, H.R. Schober, G. Vogl , Phys. Rev. B **43**, 10948 (1991).
8. C. Stassis, J. Zarestky, N. Wakabayashi, Phys. Rev. Lett. **41**, 1726 (1978).
9. Y. Chen, K.M. Ho, B.N. Harmon, Phys. Rev. B **37**, 283 (1988).
10. For a review, see B.S. Hickman, J. Mater. Sci. **4**, 554 (1969); S.L. Sass, J. Less, Common Metals **28**, 157 (1972); also see S.K. Sikka, Y.K. Vohra, R. Chidambaram, in *Progress in Material Science*, edited by B. Chalmers, J.W. Christian, T.B. Massalski (Pergamon, New York, 1982) p. 245.
11. S.C. Moss, D.T. Keating, J.D. Axe, in *Phase Transformations*, edited by L.E. Cross (Pergamon, New York, 1973) p. 179.
12. J.D. Axe, D.T. Keating, S.C. Moss, Phys. Rev. Lett. **35**, 530 (1975).
13. Y. Noda, Y. Yamada, S.M. Shapiro, Phys. Rev. B **40**, 5995 (1989).
14. A. Heiming, W. Petry, G. Vogl, J. Trampenau, H.R. Schober, J. Chevrier, O. Schärpf, Z. Phys. B **85**, 239 (1991).
15. T. Flottmann, W. Petry, R. Serve, G. Vogl, Nucl. Instr. Meth. Phys. A **260**, 165 (1987).
16. B. Dorner, *Coherent Inelastic Neutron Scattering in Lattice Dynamics*, Springer Tracts in Modern Physics **93**, (Springer, Berlin, 1984).
17. E.B. Osgood, V.J. Minkiewicz, T.A. Kitchens, G. Shirane, Phys. Rev. A **5**, 1537 (1972).
18. V.J. Minkiewicz, T.A. Kitchens, G. Shirane, E.B. Osgood, Phys. Rev. A **8**, 1513 (1973).
19. J. Meyer, G. Dolling, R. Scherm, H.R. Glyde, J. Phys. F: Metal Phys. **6**, 943 (1976).
20. F. Güthoff, W. Petry, C. Stassis, A. Heiming, B. Hennion, C. Herzig, J. Trampenau, Phys. Rev. B **45**, 2563 (1993).
21. B.L. Zhang, C.Z. Wang, K.M. Ho, D. Turner, Y.Y. Ye, Phys. Rev. Lett. **74**, 1375 (1995).
22. W. Petry, A. Heiming, J. Trampenau, M. Alba, C. Herzig, H.R. Schober, G. Vogl , Phys. Rev. B **43**, 10933 (1991).
23. J. Trampenau, W. Petry, A. Heiming, M. Alba, C. Herzig, H.R. Schober, Phys. Rev. B **43**, 10963 (1991).
24. V. Ambegaokar, J.M. Conway, G. Baym in *Lattice dynamics*, edited by R.F. Wallis (Pergamon, New York, 1965), p. 261.
25. H.R. Glyde, Can. J. Phys. **52**, 2281 (1974).